Proceedings of the ASME 2021
American Society of Mechanical Engineers Energy and Sustainability
ESASME2021
June 16-18, 2021, Virtual Conference, online

ASME ES2021-62319

RECEIVER OUTLET TEMPERATURE CONTROL FOR FALLING PARTICLE RECEIVER APPLICATIONS

Nathan Schroeder[1], Henk Laubscher[2], Brantley Mills, and Clifford K. Ho[3]

[1]MSME, R&D Mechanical Engineer, Sandia National Laboratories, P.O. Box 5800, Albuquerque, NM 87185-1127, USA, nrschro@sandia.gov, (505) 284-5767
[2]MSME, Sandia National Laboratories
[3]Ph.D., Sandia National Laboratories, (505) 844-2384, ckho@sandia.gov

ABSTRACT

Falling particle receivers (FPRs) are being studied in concentrating solar power applications to enable high temperatures for supercritical CO_2 (sCO_2) Brayton power cycles. The falling particles are introduced into the cavity receiver via a linear actuated slide gate and irradiated by concentrated sunlight. The thickness of the particle curtain associated with the slide-gate opening dimension dictates the mass flow rate of the particle curtain. A thicker, higher mass flow rate, particle curtain would typically be associated with a smaller temperature rise through the receiver, and a thinner, lower mass flow rate, particle curtain would result in a larger temperature rise. Using the receiver outlet temperature as the process variable and the linear actuated slide gate as the input parameter a proportional, integral, and derivative (PID) controller was implemented to control the temperature of the particles leaving the receiver. The PID parameters were tuned to respond in a quick and stable manner. The PID controlled slide gate was tested using the 1 MW receiver at the National Solar Thermal Test Facility (NSTTF). The receiver outlet temperature was ramped from ambient to 800°C then maintained at the setpoint temperature. After reaching a steady-state, perturbations of 15%-20% of the initial power were applied by removing heliostats to simulate passing clouds. The PID controller reacted to the change in the input power by adjusting the mass flow rate through the receiver to maintain a constant receiver outlet temperature. A goal of $\pm 2\sigma \leq 10$°C in the outlet temperature for the 5 minutes following the perturbation was achieved.

Keywords: Falling Particle Receiver, Particle Outlet Temperature Control, Particle Mass Flow Rate Control, Concentrating Solar Power

NOMENCLATURE

Q	Energy Absorbed by Particles (W)
$\dot{m}$	Mass Flow Rate (kg/s)
cp	Specific Heat of Particles (J/kg·K)
T_{out}	Outlet Temperature of Receiver (K)
T_{in}	Inlet Temperature of Receiver (K)

1. INTRODUCTION

Falling particle receivers (FPRs) utilize a solid heat transfer medium to achieve higher temperatures (>700°C) to power a more efficient Brayton power cycle for concentrating solar power (CSP) applications [1]. Particles are held in a top hopper above the receiver to be drained through a small opening, or aperture, and fall through the cavity receiver. There the particles are directly heated by concentrated sunlight as they fall through the cavity. Providing a constant receiver outlet temperature is crucial in the operation of an FPR.

The mass flow rate of the particles falling through the receiver is determined by the aperture opening at the bottom of the top hopper. An inverse relationship between the particle mass flow rate and particle outlet temperature is described by the following equation.

$$Q = \dot{m} * c_p(T_{out} - T_{in}) \quad (1)$$

Where Q is the energy absorbed by the particles (W), $\dot{m}$ is the mass flow rate (kg/s), c_p is the specific heat of the particles (J/kg·K), T_{out} is the average temperature of the particles exiting the receiver (K), and T_{in} is the average temperature of the particle entering the receiver (K). For a constant irradiance and particle inlet temperature, a decrease in the mass flow rate

increases the particle outlet temperature. Varying the aperture opening allows for the control of the particle outlet temperature through the control of the mass flow rate.

Particle mass flow rate through a 2D aperture can described by the dimension of the aperture opening and the temperature of the particles that pass through the opening. As the particle temperature increases, the friction between the particles and the walls of the opening increases. Therefore, as the particle temperature rises, the mass flow rate of particles flowing through a given aperture opening will decrease [2] [3] [4].

Peacock et al. evaluated and designed a sub-millimeter precision linear actuated slide gate attached to the top hopper to control the mass flow rate of particles with <1 kg/s accuracy. [5] A cold flow test stand with a similar system architecture is shown in Figure 1.

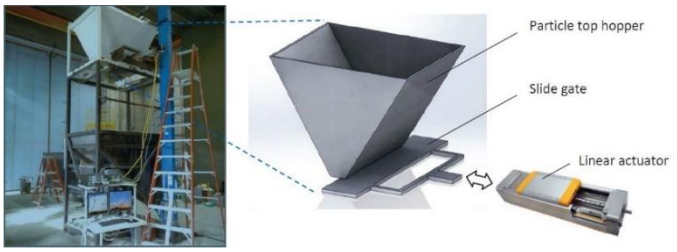

FIGURE 1: COLD FLOW TEST STAND (LEFT) WITH DETAIL OF TOP HOPPER, SLIDE GATE, AND LINEAR ACTUATOR (RIGH

Ho et al. [6] conducted on-sun tests using a proportional controller which opened and closed the slide gate to maintain the particle outlet temperature at a given setpoint. The proportional controller adjusted the slide gate opening based on the difference between the measured receiver outlet temperature and the outlet temperature setpoint. The larger the difference between the setpoint and the measured value the faster the controller open or close the slide gate to control the receiver outlet temperature. The controller was found to maintain the outlet temperature in 3 scenarios: environmental disturbances (e.g. wind, dip in DNI), adjustment of temperature setpoint, and prescribed perturbations. These prescribed perturbations are achieved by the addition or removal of heliostats associated with an increase or decrease in power incident on the particles in the receiver. While the goal of maintaining the average difference between the setpoint and the measured value below 25°C for tens to hundreds of seconds was achieved, an oscillatory particle outlet temperature was observed. The measured outlet temperature would exceed the prescribed setpoint only to overcompensate and undershoot the setpoint in a series of undamped oscillations depicted in Figure 2.

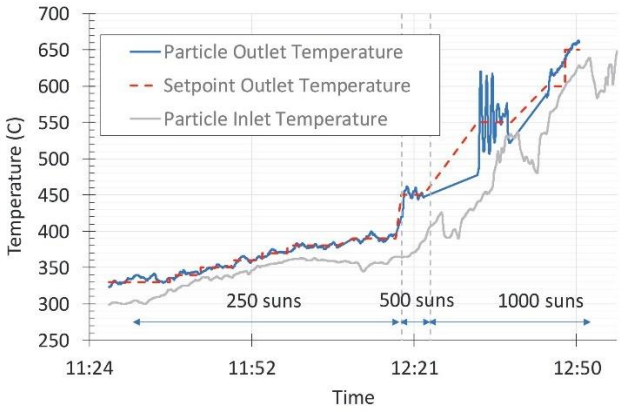

FIGURE 2: PARTICLE OUTLET TEMPERATURE CONTROL UTILIZING A PROPORTIONAL CONTROLLER [6]

Using the same test apparatus as the experiment described above, a PID outlet temperature control was implemented. The inclusion of the integral and derivative terms damps the oscillatory behavior of the system allowing for the more precise control of the receiver outlet temperature. The improved controller was considered successful if, hundreds of seconds following a 20% perturbation in the incident power, 2σ of the outlet temperature during that period was less than 10°C offset from the setpoint ($\pm 2\sigma \leq 10°C$).

2. METHOD

The FPR system used in the initial proportional control experiment and the following PID control experiment is shown in Figure 3.

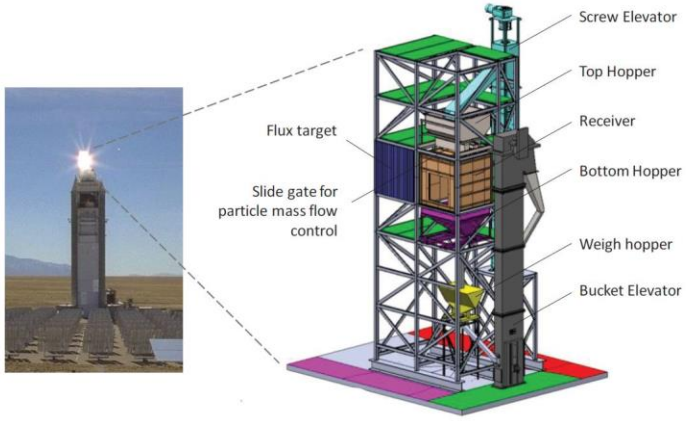

FIGURE 3: EXPERIMENTAL SETUP LOCATED AT THE NATIONAL SOLAR THERMAL TEST FACILITY [6]

The experimental setup shown above recirculates particles through the receiver. Particles are stored in the top hopper, fall through the aperture created by the linear actuated slide gate, enter the receiver to be heated by the concentrated sunlight, collect in the bottom hopper, then return to the top hopper with an auger type "Olds" particle elevator. Five type-K

thermocouples are situated at the bottom of the top hopper to measure the receiver inlet temperature along the particle curtain's width. Five funnels are situated at the bottom of the receiver, each containing one thermocouple to measure the receiver outlet temperature in a similar manner. The temperature distribution across the width of the inlet and the outlet are averaged resulting in one inlet and outlet temperature. Periodic mass flow rate measurements are taken via load cells measuring the weight of the top hopper. To take a mass flow measurement, the olds elevator is shut off halting the flow of particles into the top hopper. For a given slide gate position, particles will drain at a mass flow rate measured by evaluating the decrease in top hopper weight over time.

On a given test day the system is started by inducing particle flow through the receiver. The Olds elevator is turned on to recirculate particles and the slide gate is opened allowing particles to flow through the receiver (The slide gate will remain at a fixed position for the remainder of the startup procedure). Heliostats are positioned to focus the beam on a water-cooled flux target beside the receiver that measures the incident solar power into the receiver. The beam is then moved with a known irradiance from the flux target to the receiver to begin heating the particles. The LabView DAQ interface provides the manual and PID control for the slide gate shown in Figure 4. Slide gate limits are implemented in the LabView PID controller interface. These limits prevent the particle mass flow rate from becoming too low (which would result in the overheating of the refractory material in the receiver due to low particle curtain opacity) or too high (resulting in the draining of the particles from the top hopper as the flow out of the top hopper would outpace the input of particles by the Olds elevator). The P, I, and D parameters are input dictating the controller's response characteristics. A temperature setpoint is input and the slide gate is switched from manual control to automatic control allowing the PID controller to begin adjusting the particle mass flow rate through the receiver and thus the outlet temperature of the receiver.

FIGURE 4: PID CONTROLLER INTERFACE PANEL

To simulate perturbations such as heliostat field shading due to clouds, a fraction of the heliostats are moved from the receiver to the flux target. The incident power on the flux target is measured and compared to the initial power incident on the receiver to determine the size of the perturbation as a portion of initial power. The PID controller controls the outlet temperature for hundreds of seconds following the perturbation.

3. RESULTS AND DISCUSSION

For a given test day, the receiver inlet temperature steadily rises as more heat is supplied to the system due to the inability to reject heat from the particles for relevant irradiances. As the receiver inlet temperature rises, the change in particle temperature through the receiver must decrease to maintain the receiver outlet temperature. The PID controller steadily increases the mass flow rate at a given outlet temperature setpoint forming a quasi-steady state. Figure 5 illustrates the receiver inlet temperature rise as the receiver outlet setpoint is adjusted for an incident power of 711 kW. Slide gate position is normalized from 0-1 with 0 being fully closed and 1 being fully open. The outlet temperature set point is increased at 197 s and 659 s, and the PID controller reduces the mass flow rate through the receiver to increase the receiver outlet temperature to the new setpoint. Note that after the final change in the PID setpoint at 659 s, the receiver inlet temperature continues to rise. The PID controller compensates by increasing the mass flow rate. The difference in the receiver inlet temperature and outlet temperature is shown to decrease as the mass flow rate increases. At 1255s, the receiver slide gate is opened to its limit providing the receiver with the maximum mass flow rate. This creates a condition in which the PID controller cannot adjust the mass flow rate further causing the outlet temperature to rise beyond the prescribed setpoint.

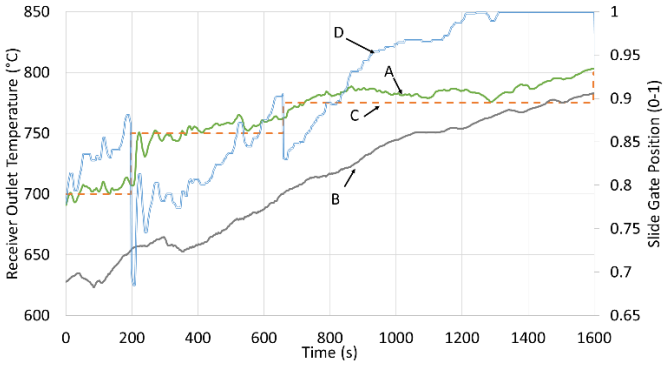

FIGURE 5: LONG TERM OUTLET TEMPERATURE CONTROL WITH ENVIRONMENTAL PERTURBATIONS WITH RECEIVER OUTLET TEMPERATURE (A), RECEIVER INLET TEMPERATURE (B), RECEIVER OUTLET TEMPERATURE SETPOINT (C), AND SLIDE GATE POSITION (D)

The oscillating behavior shown at the 197s setpoint change was a result of more aggressive PID parameters. High values for the P term with relatively low values for the I term resulted in a quicker system response but caused increased oscillation around the setpoint. The systems response can be adjusted through changes in each of the P, I, and D terms. These terms were tuned manually over the course of three test days. The system's response to a sharp perturbation was supplied to a Matlab® extension to fit a transfer function to the receiver outlet temperature's response (output) to a sharp change in the slide gate position (input). The Matlab extension generated tuned PID parameters based on the transfer function and the desired system

response. While the tuned parameters did result in a rapid and stable system response, manual fine-tuning was needed to prevent non-critically damped oscillations. The parameters that resulted in a low rise time and stable response for the perturbation tests were P = .15, I = .6, and D = .02.

To test the PID controller's response to perturbations, such as heliostat field shading due to clouds, a fraction of the heliostats were taken off of the receiver while the PID controller was maintaining the outlet temperature. Figure 6 shows three perturbation tests where the x-axis is the time from the perturbation event. The time before the event is shown as negative. To allow for the maximum adjustability of the particle mass flow rate, the test was started when the slide gate position was in the center of its limits. The PID setpoint is changed near the beginning of each test, and after a quasi-steady state is reached the perturbation is implemented. The incident power on the particles is decreased, decreasing the outlet temperature of the receiver. The PID controller compensates by reducing the mass flow rate through the receiver increasing the particle outlet temperature to the setpoint. In each of the following cases, the receiver outlet temperature was maintained after the perturbation was implemented.

Future receiver experiments will integrate a heat exchanger to reject heat from the particle loop allowing for a constant receiver inlet temperature. In this case, the change in particle temperature through the receiver (delta T) will be relatively constant. An additional control strategy was investigated using the delta T as the control feedback signal parameter. Figure 7 shows the PID response to an 18% power perturbation. Despite having started at a fully open slide gate position, resulting in the maximum flow rate, a decrease to the slide gate's lower limit resulting in the minimum flow rate, did not maintain the delta T at its setpoint. This resulted in a 30°C deviation of the measured receiver outlet temperature from the setpoint. The delta T temperature control was less robust than tests maintaining a constant change in particle temperature through the receiver resulting in increased oscillations and deviations from the setpoint. Large changes in slide gate position had less of an effect on the delta T. This may be due to a delay in measurement between the receiver inlet temperature and the receiver outlet temperature. The receiver inlet temperature is measured 6" above the linear actuated slide gate. As the slide gate closes restricting the flow of particles the delay between the receiver outlet temperature and receiver inlet temperature increases and vice versa. It is assumed that this behavior creates a variable time delay in the process variable which the PID controller cannot compensate for. In addition to the hysteresis effects, large rapid changes in the slide gate position cause cooler particles to cascade from the walls of the top hopper down into the receiver. The particles in the top hopper are flowing in "funnel flow" meaning particles at the top of the hopper are drained through the slide gate while particles at the sides of the hopper are stationary. As the mass of inventory in the top hopper decreases due to increased mass flow rate out of the hopper cooler stagnant particles along the wall begin draining momentarily decreasing the inlet temperature and thus increasing the delta T. This increased mass flow rate/increased delta T relationship is counter to the expected reaction. This behavior has less of an effect on the receiver outlet temperature control due to the lack of delay between the inlet and outlet temperature measurement. Future systems that include particle heat rejection will solely rely on the receiver outlet temperature and this behavior will not have an effect.

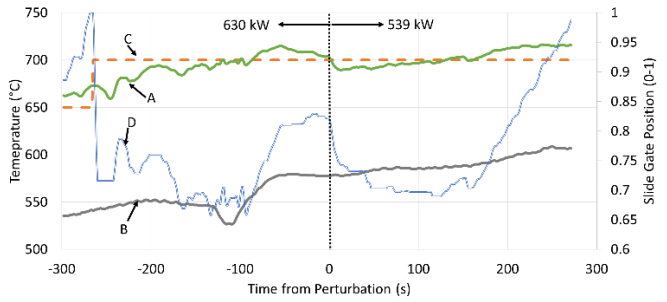

(TEST 1)

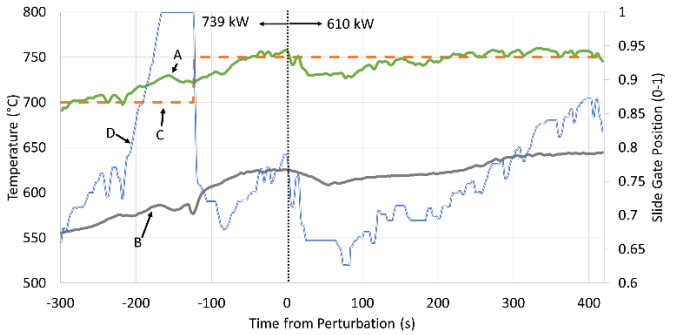

(TEST 2)

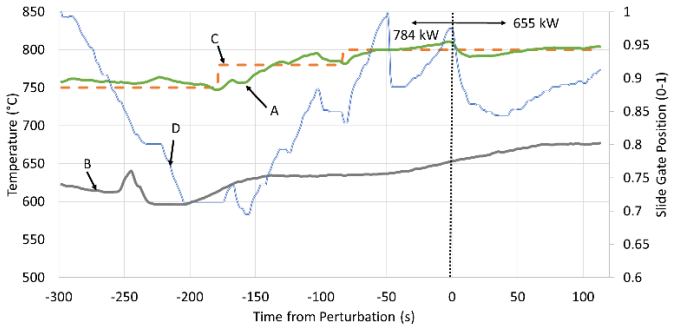

(TEST 3)

FIGURE 6: RECEIVER OUTLET TEMPERATURE RESPONSE TO PID INPUT WITH THE RECEIVER OUTLET TEMPERATURE (A), THE RECEIVER INLET TEMPERATURE (B), AND THE RECEIVER OUTLET TEMPERATURE SETPOINT (C) CORRESPONDING TO THE LEFT AXIS AND THE SLIDE GATE POSITION (D) CORRESPONDING TO THE RIGHT AXIS

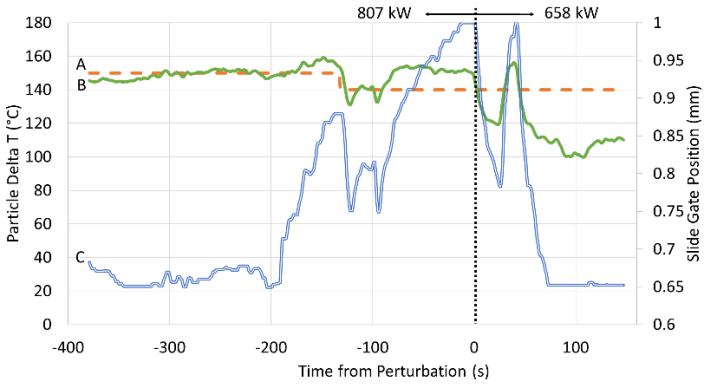

FIGURE 7: SLIDE GATE RESPONSE TO A PERTURBATION USING A DELTA T INPUT PARAMETER INCLUDING THE PID SETPOINT (A) AND DELTA T THROUGH THE RECEIVER (B) CORRESPONDING TO THE LEFT AXIS AND THE SLIDE GATE POSITION (C) CORRESPONDING TO THE RIGHT AXIS

Table 1 summarizes the perturbation experiments conducted with both the outlet temperature and delta T control strategy. All outlet temperature perturbation tests resulted in the successful maintenance of the receiver temperature ±2σ≤10°C criterion. The delta T control strategy did not result in the successful maintenance of the change in temperature through the receiver when exposed to an 18% perturbation. It is important to note that despite having the largest perturbation the next largest test perturbation test, 17%, for the outlet temperature control began with the slide gate position further from its limits, reducing the adjustability available when compared to the delta T test.

TABLE 1: PID CONTROLLED OUTLET TEMPERATURE TEST MATRIX

	Test 1 (Outlet Temp)	**Test 2 (Outlet Temp)**	**Test 3 Outlet Temp)**	**Test 4 (ΔT)**
Prescribed Temperature Setpoint (°C)	700	750	800	140
Initial Incident Power (kW)	630	739	784	807
Perturbation (% of Initial Power)	15%	17%	16%	18%
Length of Time used for Criterion (s)	271	418	113	147
Average Temperature During Sample Period (°C)	702	746	799	118
2σ	1.05	.92	.93	2.53
Setpoint-(μ±2σ) (°C)	1.4-3.5	2.1-4.0	.1-2.0	19.8-24.8
±2σ≤10°C Criterion Satisfied?	Yes	Yes	Yes	No

The PID controller was also tested on a day with dense high clouds shown in Figure 8:. The peak DNI recorded between clouds was 840 W/m^2 with dips down to 65 W/m^2 as the clouds passed over the heliostat field. The PID controller maintained the average receiver outlet temperature close to the setpoint, but insufficient irradiance while the field was shaded caused the outlet temperature to decrease. Between clouds, during periods of high irradiance, the receiver outlet temperature overshoots the setpoint. The slide gate opens to allow for the maximum flow rate of particles, but the maximum mass flow is not sufficient to maintain the setpoint temperature. The inverse is true for periods of low irradiance. A heliostat defocusing strategy used a PID controller to maintain the particle outlet temperature during related testing in the same test campaign. The defocusing PID controller adjusted heliostats radially outward from the receiver, decreasing the incident power thus decreasing the particle outlet temperature. A combination defocusing and receiver slide gate outlet temperature controller is being considered to allow for system operation for larger environmental perturbations.

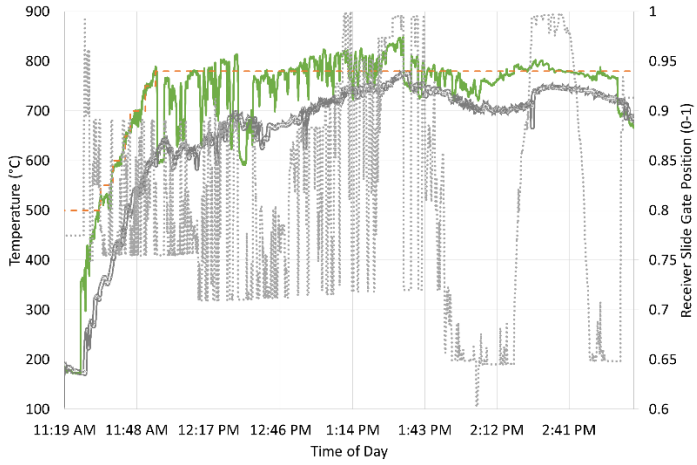

(A)

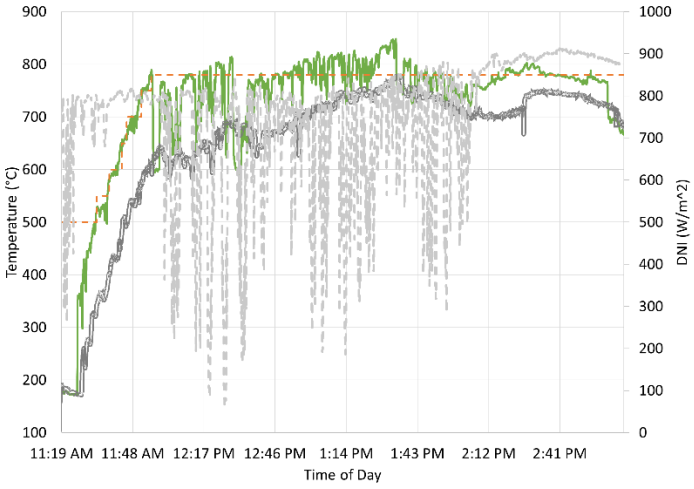

(B)

FIGURE 8: PID CONTROLLED OUTLET TEMPERATURE DURING A CLOUDY DAY WITH LIGHT DOTTED LINES IN (A) REPRESENTING SLIDE GATE POSITION AND LIGHT DOTTED LINES IN (B) REPRESENTING DNI CORRESSPONDING TO THE RIGHT AXIS. HEAVY DOTTED LINES INDICATE PID SETPOINT, THE SINGLE SOLID LINE REPRESENTS RECEIVER OUTLET TEMPERATURE, AND THE DOUBLE SOLID LINE THE RECEIVER INLET TEMPERATURE CORRESPONDING THE LEFT AXIS

Specific input conditions have been found to invert the mass flow rate/outlet temperature relationship. A test conducted with high receiver inlet temperatures (>750°C) and low incident power (500 kW) created a scenario in which a decrease in mass flow rate results in a decrease in receiver outlet temperature. At higher inlet temperatures the advective losses are increased as the hotter air in the receiver forms a larger thermal gradient with the ambient air outside the receiver. [7]. It is assumed that the inverse behavior is caused by a decrease in the curtain's absorptivity with a simultaneous increase in thermal losses. At higher mass flow rates air entrained by the curtain creates a gathering effect 1-2m from the curtain origin, compressing the curtain thickness as air surrounding the curtain is pulled toward it. This increases the curtain's solids fraction [8]. At lower mass flow rates this behavior has a diminished effect allowing for greater particle dispersion, decreasing the solids fraction. Discrete particles lose more heat due to convection than particles that are entrained in a curtain [9]. Particle curtain absorptivity is also greater than discrete particle absorptivity as the curtain has a light trapping effect. Total particle power absorbed (absorbed energy – reradiated energy) not including convective losses has been shown to decrease with decreased flow rate/particle volume fraction [10]. With increased thermal losses at high temperatures, compounding the effects of decreased curtain absorptivity and increased thermal losses due to convection and radiation may explain the inverse mass flow rate/outlet temperature relationship. Following this discovery experiments we conducted with high inlet temperatures (>750°C) and high incident power (>700kW). With a higher ratio of incident power to thermal losses, the inverse mass flow rate/outlet temperature relationship was not present.

4. CONCLUSION

A PID controlled slide gate implemented to maintain the receiver outlet temperature was tuned and tested. The controller maintained the receiver outlet temperature at the desired set point through changes in setpoint, environmental disturbances (e.g. wind/variations in DNI), and prescribed perturbations in incident power. Using an outlet temperature control strategy, the PID controller was able to maintain the receiver outlet temperature at $\pm 2\sigma \leq 10°C$ after a 17% decrease in incident power for 418 seconds following the event. Using the controller to maintain a set change in temperature through the receiver failed to meet the criteria for a successful perturbation test. The PID controller was tested in a "real-world" condition with high dense clouds. While the PID controller maintained the outlet temperature at the setpoint when sufficient power was available, large changes in DNI and thus incident power requires additional forms of outlet temperature control.

ACKNOWLEDGEMENTS

This work was funded in part or whole by the U.S. Department of Energy Solar Energy Technologies Office under Award Number 34211. This report was prepared as an account of work sponsored by an agency of the United States Government. Neither the United States Government nor any agency thereof, nor any of their employees, makes any warranty, express or implied, or assumes any legal liability or responsibility for the accuracy, completeness, or usefulness of any information, apparatus, product, or process disclosed, or represents that its use would not infringe privately owned rights. References herein to any specific commercial product, process, or service by trade name, trademark, manufacturer, or otherwise does not necessarily constitute or imply its endorsement, recommendation, or favoring by the United States Government or any agency thereof. The views and opinions of the authors expressed herein do not necessarily state or reflect those of the United States Government or any agency thereof.

Sandia National Laboratories is a multimission laboratory managed and operated by National Technology and Engineering Solutions of Sandia, LLC., a wholly-owned subsidiary of Honeywell International, Inc., for the U.S. Department of Energy's National Nuclear Security Administration under contract DE-NA0003525.

REFERENCES

[1] C. K. Ho, "A Reveiw of High-Temperature Particle Receivers for Concentrating Solar Power," *Applied Thermal Egineering,* vol. 109 Part B, pp. 958-969, 2016.

[2] K. J. Albreicht and C. K. Ho, "High-Temperature Flow Testing and Heat Transfer for a Moving Pack-Bed Particle/sCO2 Heat Exchanger," in *SolarPACES*, Santiago, Chile, 2017.

[3] W. A. Beverloo, H. A. Leniger and J. Vandevelde, "The Flow of Granular Solids Through Orifices," *Chemical Engineering Science,* vol. 15, no. 3-4, pp. 260-&, 1961.

[4] A. Janda, I. Zuriguel and D. Maza, "Flow Rate of Particles through Apertures Obtained from Self-Similar Density and Velocity Profiles," *Phys Rev Lett,* vol. 108, p. 109, 2012.

[5] G. Peacock, C. K. Ho, J. M. Christian and D. Ray, "Automated Particle Mass-Flow Control System for High-Temperature Falling Particle Receivers," in *SolarPACES*, Santiago, Chile, 2017.

[6] C. K. Ho, G. Peacock, J. M. Christion, K. Albrecht, J. E. Yellowhair and D. Ray, "On-sun testing of a 1 MWt Particle Receiver with automated particle mass-flow and Temperature Control," in *SolarPACES*, Daegu, South Korea, 2019.

[7] B. Mills, R. Shaeffer, C. K. Ho and L. Yue, "Modeling the Thermal Performance of Falling Particle Receiver Subject to External Wind," in *ESASME*, Bellevue, Washington, USA, 2019.

[8] C. K. Ho, J. M. Christian, D. Romano, J. Yellowhair, N. Siegle, L. Savoldi and R. Zanino, "Charaterization of Particle Flow in a Free-Falling Solar Particle Receiver," *Journal of Solar Energy Engineering,* vol. 139, 2017.

[9] J. Hruby, R. Steeper, G. Evans and C. Crowe, "An Experimental and Numerical Sutdy of Flow and Covective Heat Transfer in a Freely Falling Curtain of Particles," *Journal of Fluids Engineering,* vol. 110, pp. 172-181, 1988.

[10] A. Kumar, J.-S. Kim and W. Lipinski, "Radiation Absorption in a Particle Curtain Exposed to Direct High-Flux Solar Irradiation," *Journal of Solar Energy Engineering ,* vol. 140, 2018.